tvst

DOI: 10.1167/tvst.2.4.1

Clinical Trials

Factors Affecting Perceptual Threshold in Argus II Retinal Prosthesis Subjects

A. K. Ahuja[1,3] ✉, J. Yeoh[2], J. D. Dorn[1], A. Caspi[1], V. Wuyyuru[1], M. J. McMahon[1], M. S. Humayun[3], R. J. Greenberg[1], L. daCruz[2], and Argus II Study Group

[1]Second Sight Medical Products, Inc., Sylmar, CA
[2]Moorfields Eye Hospital, London, UK
[3]Doheny Eye Institute, Keck School of Medicine, Los Angeles, CA

Correspondence: Ashish Ahuja, 1130 South Flower St. #120, Los Angeles, CA 90015, e-mail: ashish.ahuja@me.com

Received: 28 May 2012
Accepted: 31 January 2013
Published: 11 April 2013

Keywords: retinal prosthesis; retinal degeneration; retinitis pigmentosa

Citation: Ahuja AK, Yeoh J, Dorn JD, et al. Factors affecting perceptual thresholds in Argus II retinal prosthesis subjects. Trans Vis Sci Tech. 2013;2(4):1, http://tvstjournal.org/doi/full/10.1167/tvst.2.4.1, doi:10.1167/tvst.2.4.1

Purpose: The Argus II epiretinal prosthesis has been developed to provide partial restoration of vision to subjects blinded from outer retinal degenerative disease. Participants were surgically implanted with the system in the United States and Europe in a single arm, prospective, multicenter clinical trial. The purpose of this investigation was to determine which factors affect electrical thresholds in order to inform surgical placement of the device.

Methods: Electrode–retina and electrode–fovea distances were determined using SD-OCT and fundus photography, respectively. Perceptual threshold to electrical stimulation of electrodes was measured using custom developed software, in which current amplitude was varied until the threshold was found. Full field stimulus light threshold was measured using the Espion D-FST test. Relationships between electrical threshold and these three explanatory variables (electrode–retina distance, electrode–fovea distance, and monocular light threshold) were quantified using regression.

Results: Regression analysis showed a significant correlation between electrical threshold and electrode–retina distance ($R^2 = 0.50$, $P = 0.0002$; $n = 703$ electrodes). 90.3% of electrodes in contact with the macula ($n = 207$) elicited percepts at charge densities less than 1 mC/cm^2/phase. These threshold data also correlated well with ganglion cell density profile ($P = 0.03$). A weaker, but still significant, inverse correlation was found between light threshold and electrical threshold ($R^2 < 0.52$, $P = 0.01$). Multivariate modeling indicated that electrode–retina distance and light threshold are highly predictive of electrode threshold ($R^2 = 0.87$; $P < 0.0005$).

Conclusions: Taken together, these results suggest that while light threshold should be used to inform patient selection, macular contact of the array is paramount.

Translational Relevance: Reported Argus II clinical study results are in good agreement with prior in vitro and in vivo studies, and support the development of higher-density systems that employ smaller diameter electrodes. (clinicaltrials.gov identifier: NCT00407602)

Introduction

The Argus II retinal prosthesis system (Second Sight Medical Products, Inc., Sylmar, CA) is aimed at partially restoring vision to people blinded by outer retinal degenerative diseases such as retinitis pigmentosa (RP). In these diseases, while the photoreceptors are compromised and there is anatomical remodeling of the remnant retina[1] postmortem anatomical studies of patients with RP and AMD[2,3] have found that a number of bipolar and ganglion cells survive. Multiple acute and chronic studies in such patients have shown that electrical stimulation of the retina can elicit percepts (phosphenes) by placing an electrode array either subretinally[4,5] (between the outer and inner retina) or epiretinally[6] (in contact with the vitro-retinal boundary). The largest subretinal and epiretinal prosthesis clinical studies are currently being conducted by Retina Implant AG (Reutlingen, Germany) and Second Sight Medical Products, Inc., respectively. Both systems have shown evidence that

some restoration of vision is possible for blind patients, allowing some subjects to read high-contrast, large font letters and words.[7,8] In this paper we restrict our investigation to the Second Sight Medical Products Inc. Argus II System clinical trial since it is the largest chronic visual prosthesis study to date.

The Argus II System consists of a surgically implanted 60-channel stimulating microelectrode array, an inductive coil link used to transmit power and data to the internal portion of the implant, an external video processing unit (VPU), and a miniature camera mounted on a pair of glasses. The video camera captures a portion of the visual field and relays the information to the VPU. The VPU digitizes the signal in real-time, applies a series of image processing filters, down samples the image to a 6×10 pixelated grid, and creates a series of stimulus pulses based on pixel grayscale values and look up tables customized for each subject. The stimulus pulses are delivered to the microelectrode array via an inductive radio frequency (RF) coil link and the application-specific circuitry. It has been shown that the Argus II system affords most implanted subjects with some spatial vision (Ahuja A, et al. *IOVS*. 2010;51:ARVO E-Abstract 4322), and that these subjects can perform better with the system on compared with off in door-finding and line-tracking orientation and mobility tests,[9] and in spatial-motor object localization and direction of motion test using high contrast stimuli (McMahon MJ, et al. *IOVS*. 2009;50:ARVO E-Abstract 4589; Ahuja A, et al. *IOVS*. 2009;50:ARVO E-Abstract 4590).[10]

The process of creating the aforementioned subject-specific look up tables that convert grayscale to current amplitude value for each electrode is part of system fitting. System fitting is based on a host of variables, electrical stimulus threshold of each electrode being chief among them. Low electrical thresholds are desirable for many reasons. In studies of cortical stimulation with penetrating probes a charge density limit of 0.35 mC/cm^2/phase was imposed to ensure safety of neural tissue,[11] and to avoid corrosion of stimulating electrode material.[12] More recent studies on electrodeposited platinum grey used in the Argus II implant show that acute stimulation is safe up to 1 mC/cm^2/phase.[13,14] This chemistry has the advantage of increased surface area and porosity so that maximal charge can be delivered safely, while still maintaining mechanical stability of the film. Low charge pulses also minimize power requirements of the system, and should also allow for more focal percepts due to localization of the electric field.[15] For these reasons low electrical thresholds should increase both the number of electrodes that can elicit percepts and the effective dynamic range of the system.

Determining which factors affect electrical thresholds may allow informed patient selection and better surgical placement of the multi-electrode array. An investigation of such factors was performed in subjects implanted with the first generation (Argus I) 4×4 electrode retinal prosthesis implant.[16] Using time-domain optical coherence tomography (OCT), it was shown that electrical threshold decreases with electrode–retina distance. Here, this type of analysis of predictive factors is extended into the larger cohort of subjects implanted with the Argus II retinal prosthesis by quantifying the effect of electrode–retina distance, macular placement, and dark-adapted light threshold on electrical threshold.

Methods

Selection Criteria for Surgical Implantation

Blind subjects with severe to profound RP were implanted with the Argus II prosthesis as part of a phase I feasibility study (clinicaltrials.gov identifier: NCT00407602; active) at multiple clinical sites worldwide. Those centers were: Puerta de Hierro Centro Medico (Guadalajara, Mexico); The Doheny Eye Institute at the University of Southern California (Los Angeles, CA); Wilmer Eye Institute at the Johns Hopkins School of Medicine (Baltimore, MD); University of California at San Francisco (San Francisco, CA); The Greenville Surgical Center (Dallas, TX); Hôpitaux Universitaires de Genève (Geneva, Switzerland); Centre Hospitalier National d'Ophtalmologie des Quinze-Vingts (Paris, France); Moorfields Eye Hospital (London, UK); The Edward S. Harkness Eye Institute at Columbia University (New York, NY); Wills Eye Insititute at the University of Pennsylvania (Philadelphia, PA). All data presented here were collected at these clinical sites, with the exception of sites in Dallas, New York, and Philadelphia where psychophysical data were collected at The Retina Foundation of the Southwest (Dallas, TX), Lighthouse International (New York, NY), and The Scheie Eye Institute at The University of Pennsylvania (Philadelphia, PA), respectively. The study was approved by institutional review boards and ethics committees at each site, and respected the tenets of the Declaration of Helsinki. Informed consent was obtained from all subjects.

Table 1. Details of Age at Time of Implant, Eye Implanted, Days Since Implant (at Time of Submission), and Self-Reported Duration of Blindness

Subject	Age at Implantation	Implanted Eye	Days Implanted	Years Blind (Self-Reported)
11-001	55	OD	990	26
11-002	61	OD	948	21
12-001	52	OD	969	23
12-002	60	OD	981	–
12-003	75	OD	981	36
12-004	52	OD	969	23
14-001	56	OS	239	–
15-003	77	OD	687	58
17-002	66	OD	956	62
51-001	70	OD	676	61
51-002	51	OD	676	21
51-003	72	OD	627	52
51-005	55	OD	333	36
51-006	60	OD	305	51
51-007	63	OD	249	25
51-009	45	OD	193	15
52-001	50	OD	262	23
52-003	60	OD	199	30
61-004	59	OD	331	21
61-005	49	OD	268	32
71-001	60	OD	740	40
71-003	27	OS	353	23

Some data regarding numbers of self-reported years blind not available due to gradual loss of vision.

All implanted subjects had bare light perception (BLP) prior to surgery, and with the device off at the time of the latest clinical follow up. No subject had a recordable visual acuity prior to surgery, all scored worse than the lowest level of 2.9 logMAR (i.e., worse than 20/15,887) on a four alternative forced choice (4-AFC) square wave grating test (details of this psychometric test have been described elsewhere[17]). Unless mentioned otherwise, data from 22 subjects were considered in this investigation (Table 1). Cases in which a smaller subset of this group were considered due to (1) lack of sufficient retinal imaging data, or (2) required full field stimulus light threshold test equipment on site, are noted in relevant *Methods* or *Results* sections.

Description of Device

The Argus II system consists of an active implantable device surgically implanted on and in the eye, and an external unit worn by the user (Fig. 1). The external unit consists of a small camera and transmitter mounted on glasses and a video processor and battery worn on the belt. The implanted portion consists of a receiving and transmitting coil and an electronics case (which are fixed to the sclera outside of the eye), and an electrode array (60 electrodes; 200-μm diameter each) that is secured to the surface of the retina inside the eye by a retinal tack. The electrode array is connected to the electronics case by a metalized polymer cable that penetrates the sclera in the pars plana. The camera captures video and sends the information to the processor, which converts the image to electronic signals that are then sent to the transmitter on the glasses. The implanted receiver wirelessly receives these data and sends the signals to the electrode array via a small cable, where electrical stimulation pulses are emitted. The controlled electrical stimulation of the retina induces cellular responses in the retina that travel through the optic nerve to the visual cortex and result in visual percepts.

Determination of Electrode–Retina Distance using Optical Coherence Tomography

Spectral-domain OCT (SD-OCT) images were obtained using the systems available at each clinical

Figure 1. The Argus II system. An illustration showing the surgically implanted stimulating microelectrode array, and inductive coil telemetry link of the Argus II system (*left*). The external portions of the system consist of a VPU (*middle*), and a miniature camera mounted on a pair of glasses (*right*). The glasses contain the half of the inductive link transmitting both power and data to the intraocular portion of the implant. (Reproduced from Ahuja AK, Dorn JD, Caspi A, et al. Blind subjects implanted with the Argus II retinal prosthesis are able to improve performance in a spatial-motor task. Br. J Ophthalmol. 2011;95:539-43, copyright 2011, with permission from BMJ Publishing Group Ltd.).

site RTVue100 OCT (Optovue, Fremont, CA); Topcon 3D-OCT 1000 (Topcon Inc., Tokyo, Japan); Cirrus HD OCT (Carl ZeissMeditec, Inc., San Francisco, CA); Spectralis OCT (Heidelberg Engineering, Heidelberg, Germany). When imaging subjects implanted with the Argus II retinal prosthesis implant, metal electrodes of the multi-electrode array reflect light from the source, casting shadows on the retinal image in areas directly below them, whereas the largely transparent polymer regions between these electrodes allow light to pass (Fig. 2). Shadows on the OCT image b-scan along with corresponding registered fundus images showing the scan line location allow for distance measurements to be made between the electrodes and the inner limiting membrane (ILM) of the retina.[16]

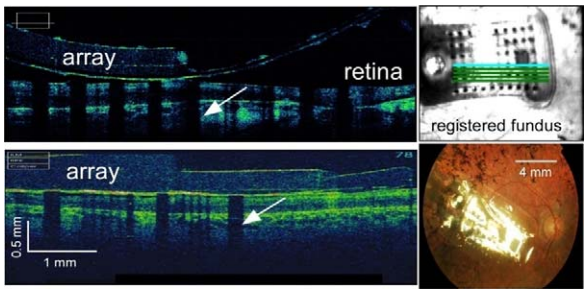

Figure 2. Spectral-domain optical coherence tomography (SD-OCT) with registered fundus images allow for electrode–retina distance to be measured. SD-OCT b-scans taken across portions of 12-001′s electrode array (*top left*) using a Cirrus SD-OCT and 52-001′s array (*bottom left*) using a Topcon SD-OCT. The metal electrodes block light from the scanning light source, casting shadows (*white arrows*) on the retinal image. Electrode shadows along with corresponding registered fundus images (*top right*) allow for the measurement of electrode–retina distance. (*Bottom right*) Fundus image of subject 61-003.

It was not possible to make accurate electrode–retina distance measurements for all electrodes due to the following reasons. Severe nystagmus of many blind subjects precluded accurate registration of each distance with a specific electrode and associated threshold. The primary system used (Heidelberg Spectralis SD-OCT) employed an eye-tracking algorithm that timed out after 3 minutes, giving insufficient time for scanning fatigued subjects. Finally, poor signal-to-noise ratio (SNR) due to opacification of the anterior optics or the vitreous cavity also lowered the number of subjects included in this analysis. There is no reason to believe that these criteria excluded electrodes preferentially. Given logistical constraints the data present a random and significant sample of electrode distances among all 22 subjects.

Distance measurements were made using the caliper measurement tool on the OCT system software. Occasionally measurements were not made on the system at the clinical site. In these cases, distances were measured in exported individual b-scans using Canvas X software (v. 10.4.9; ACD Systems, Seattle, WA) and the values were calibrated using the length of reference markers. Variability was assessed by comparing the measurements made by two different authors (AA and JY) on the same subset of data; two different statistical tests were run on these data to show distance measurements were accurate. Least squares fitting on both sets of measurements were well correlated ($R^2 = 0.91$; $P <$

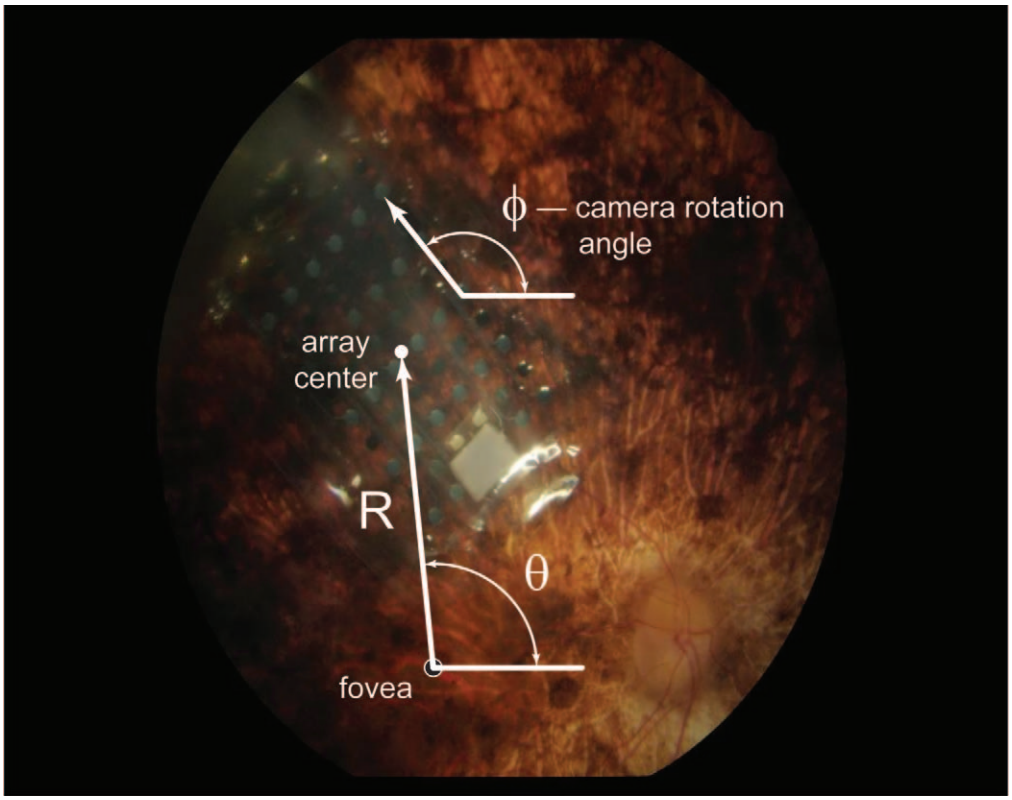

Figure 3. A fundus photograph illustrating the variables used to calculate electrode–fovea distance and orientation. ϕ is the angle of the array long axis relative to horizontal. θ is the angle between the fovea to array (vector R) and the horizontal.

0.0001) with a best-fit linear regression slope of 0.96. (Note that perfect agreement between readers would yield a slope of 1.)

Determination of Electrode–Fovea Distance using Fundus Photography

The distances between electrodes and the fovea were determined by analyzing fundus photographs of implanted eyes (Fig. 3). Stereoscopic color fundus photos centered on the array center were obtained using systems available at each clinical site. Foveal location was determined using previously published coordinates with respect to the optic disc (15.5 ± 1.1° temporal, 1.5 ± 0.9° inferior; n = 104 eyes of normals[18]), with the conversion factor that 1° of visual angle subtends 288 μm on the retinal surface.[19] It was difficult to visualize foveal pit location using OCT because (1) array apposition changed local topology, and (2) degeneration has been shown to compromise laminar structure and morphology in RP patients.[20,21] Therefore, it was not possible to use these scans and registered fundus images to determine location.

Measurements were made between the array center and the fovea using Canvas X software (v. 10.4.9). The known electrode–electrode spacing of the array served as a calibration for measurement. Based on the location of the fovea with respect to the array center and on the angle of the array rotation with respect to the horizontal, all electrode–fovea distances were calculated using Matlab (MathWorks, Natick, MA). In order to partially account for the confounding variable of differences in electrode–retina distance, the mean geometric electrode–fovea distance (defined as the hypotenuse of the triangle defined by electrode–retina and electrode–fovea distances) was calculated.

Taken together the foveal pit, the parafovea, and the perifovea constitute the macula. While yellow screening pigments allow for visualization of macular extent in normal eyes, it is difficult to discriminate the macula-periphery boundary in these subjects because of the characteristic pigmentary deposits associated with RP. Here electrodes were considered to be in the macula if they were within 3 mm of fovea centralis.

Electrical Threshold

Perceptual threshold to stimulation of individual electrodes was measured using custom developed

software. Each stimulus presentation consisted of a 250 ms duration train of cathodic first, biphasic pulses delivered at a frequency of 20 Hz (i.e., five pulses/train); the pulsewidth of each phase of individual pulses within a train was 0.45 ms and there was no interphase interval (i.e., the total biphasic pulsewidth was 0.90 ms).

Stimulation thresholds were measured with a procedure that is a combination of the method of constant stimuli (MOC), in which predetermined current amplitudes are presented randomly, and an adaptive method of threshold estimation, in which current amplitudes to be tested are determined based on previous responses. We have found that this hybrid threshold algorithm quickly converges to a measurement compared with standard MOC since the latter requires the full psychometric function be measured.

Up to six different electrodes were tested in a single experimental run; in each trial, an audio prompt was followed by either stimulation of one of the electrodes, selected randomly from the set, or no stimulation, in the case of a catch trial. Subjects used a keypad to respond "yes" if a percept was seen, or "no" if it was not. Trials were divided into blocks, up to five blocks of 12 trials were completed for each electrode group. After the first block, a maximum likelihood algorithm determined the range of the next block of stimulation values for each electrode group, based on all previous responses. If the confidence interval (CI) of the estimated threshold of an electrode group was narrowed to a level of 95%, trials for that electrode terminated, but trials on the other electrodes continued through a maximum of five blocks. Stimulus pulse amplitude ranged from 4 to 677 μA. In a full run, 32 catch trials (i.e., an audio prompt with no stimulus) were interspersed over the five presentation blocks. False alarm rates greater than 20% were an indication of unreliable results; data from runs with higher false alarm rates were removed from analysis and the runs were repeated until reliable data were obtained.

Despite the efficiency of this hybrid threshold technique, it was still too time consuming to attempt to measure thresholds for each electrode in each array. Therefore, instead of running the hybrid threshold algorithm on each electrode, we began by stimulating each electrode at the maximum current amplitude (677 μA corresponding to 1 mC/cm^2/phase) three times and recording which stimulated electrodes resulted in at least one percept. We were then able to run the full threshold experiment only on those electrodes likely to result in measurable thresholds.

Full Field Stimulus Light Threshold

Dark-adapted light thresholds of implanted and fellow eyes to full field white light stimuli were measured using the Espion D-FST test (Diagnosys LLC, Littleton, MA) within the commercially available E^2 clinical electrophysiology software package (version 5.0; Diagnosys LLC). An Espion ColorDome Ganzfeld and the E^2 console (both, Diagnosys LLC) were used for stimulus presentation. A similar test has also been used to quantify visual sensitivity in gene therapy studies aimed at restoring function in those blinded by Leber's Congenital Amaurosis (LCA).[22,23] In a comparative investigation, both of these tests have been shown to output similar light thresholds.[24] The Espion stimulus flash duration and maximum luminance were 4 ms and 3000 (cd)(s)/m^2, respectively; inter-stimulus duration was 5 seconds. Threshold was defined as the stimulus intensity corresponding to the midpoint of the psychometric function. The 0 dB point was set to 3 (cd)(s)/m^2 and employed a staircase method with 16 reversals required for convergence. Prior to testing, subjects' eyes were dilated and dark-adapted for 30 minutes. Monocular thresholds were obtained by patching the other eye during testing. The system was off during all tests so that only native light sensitivity was measured. Light thresholds were reported for subjects at sites equipped with the required Espion software needed to run the D-FST test ($n = 11$ subjects). Since multiple tests would lead to light adaptation, measuring repeatability within a session was difficult. However, monocular dark-adapted light thresholds of implanted and fellow eyes were strongly correlated ($R^2 = 0.86$; $P < 0.0001$; $n = 11$ subjects) providing some validation of the method.[25]

Data Analysis

Electrode threshold data and analyzed images for individual subjects were both time matched to the extent possible given subject availability and clinical trial protocol schedule (the maximum time lapse between imaging and threshold data collection was 6 weeks.) Three different threshold measures are used when regressing against explanatory variables: mean threshold, percentage of available electrodes with thresholds below 233 μA (corresponding to a 0.35 mC/cm^2/phase charge density limit), and the percentage of available electrodes with thresholds below 677 μA (corresponding to a 1.0 mC/cm^2/phase charge

Table 2. Linear Regression was Performed using a Standard Least Squares Method to Quantify the Extent to which Explanatory Variables Could Predict Threshold Response Measures

	Mean Retinal Distance (μm)		Mean Foveal Distance (μm)		Light Threshold (cd)(s)/m^2 (Implanted Eye)		Light Threshold (cd)(s)/m^2 (Fellow Eye)	
	R^2	P	R^2	P	R^2	P	R^2	P
Mean electrode threshold (μA)	0.50	0.0002	0.49	0.007	0.52	0.01	0.35	0.06
Electrodes (%) threshold <0.35 mC/cm^2	0.52	<0.0001	0.65	0.0009	0.40	0.04	0.22	0.15
Electrodes (%) threshold <1 mC/cm^2	0.26	0.01	0.71	0.0003	0.10	0.35	0.03	>0.2

Coefficient of determination (R^2) and significance of the trend (P-value) are given for each of the individual predictors. With the exception of Electrodes (%) threshold less than 1 mC/cm^2 and light threshold of implanted eyes, all measures of threshold showed a significant relationship when regressed against retinal distance, foveal distance, and light threshold of implanted eyes.

density limit). Mean threshold is the average value of all electrodes with a measurable threshold, and, therefore, does not account for electrodes with thresholds above the maximum charge density limit(s). Both measures of the percentage of available electrodes with thresholds, however, do take these electrodes into account.

Data were analyzed and plots were generated using Matlab 7.0, Igor Pro 6.1 (WaveMetrics, Lake Oswego, OR), Microsoft Excel 2007 (Microsoft, Seattle, WA), and JMP 8.0 (SAS Institute, Cary, NC) statistical analysis software Images were analyzed using Canvas Illustrator X software. The normative ganglion cell density values were extracted from Curcio and Allen's "The topology of ganglion cells in the human retina" using the software package PlotDigitizer.[26]

There were two primary reasons electrode or subject data were omitted from some analysis. Severe nystagmus or ocular opacification made it difficult to register some electrodes with corresponding shadows in SD-OCT b-scans, thereby limiting the number of electrodes included in electrode–retina distance regression analysis. The lack of calibrated D-FST light threshold setups at all clinical sites pre- and post-implantation precluded the inclusion of all subjects in D-FST regression analysis. Linear ($y = ax + b$) and square of distance ($y = a + bx^2$) regression analyses weighted by individual subject electrode count were performed using a Sum of Least Squares Method. Bivariate regression analysis was performed on explanatory variable pairs as well. In order to further investigate the effect of macular placement on mean threshold without being affected by the confounding factor of electrode-retina distance, some analyses considered only electrodes that were in contact with tissue (as noted). A 95% CI was used as a cutoff for statistical significance ($P < 0.05$).

Results

The mean electrode threshold across all subjects was 206.5 ± 6.3 μA ($n = 703$ electrodes) and the mean electrode–retina distance was 179.6 ± 6.5 μm ($n = 1013$ electrodes). Goodness-of-fit coefficients for linear ($y = 0.56x + 112$) and square of distance ($y = 7.8 \times 10^{-4}\ x^2 + 158$) fits performed on individual subjects were not statistically different (two-tailed paired Student's t test, $P > 0.15$). While only electrodes with measureable thresholds can be included in this analysis, mean electrode–retina distance also correlated well with the percentage of available electrodes with thresholds below the 0.35 mC/cm^2 limit ($R^2 = 0.52$; $P < 0.0001$) and the percentage below the 1 mC/cm^2/phase limit ($R^2 = 0.26$; $P = 0.01$).

The same analysis was also performed mean electrode–fovea distance data and on D-FST light threshold data (implanted and fellow eyes) in order to determine if significant relationships existed between these explanatory variables and any measure of threshold (Fig. 4; Table 2). Light sensitivity proved to be a predictor of threshold, as implanted eye light threshold correlated well with mean electrode threshold ($P < 0.02$) and the percentage of electrodes with thresholds below 0.35 mC/cm^2 ($P < 0.05$). Light threshold of the fellow eye did not significantly

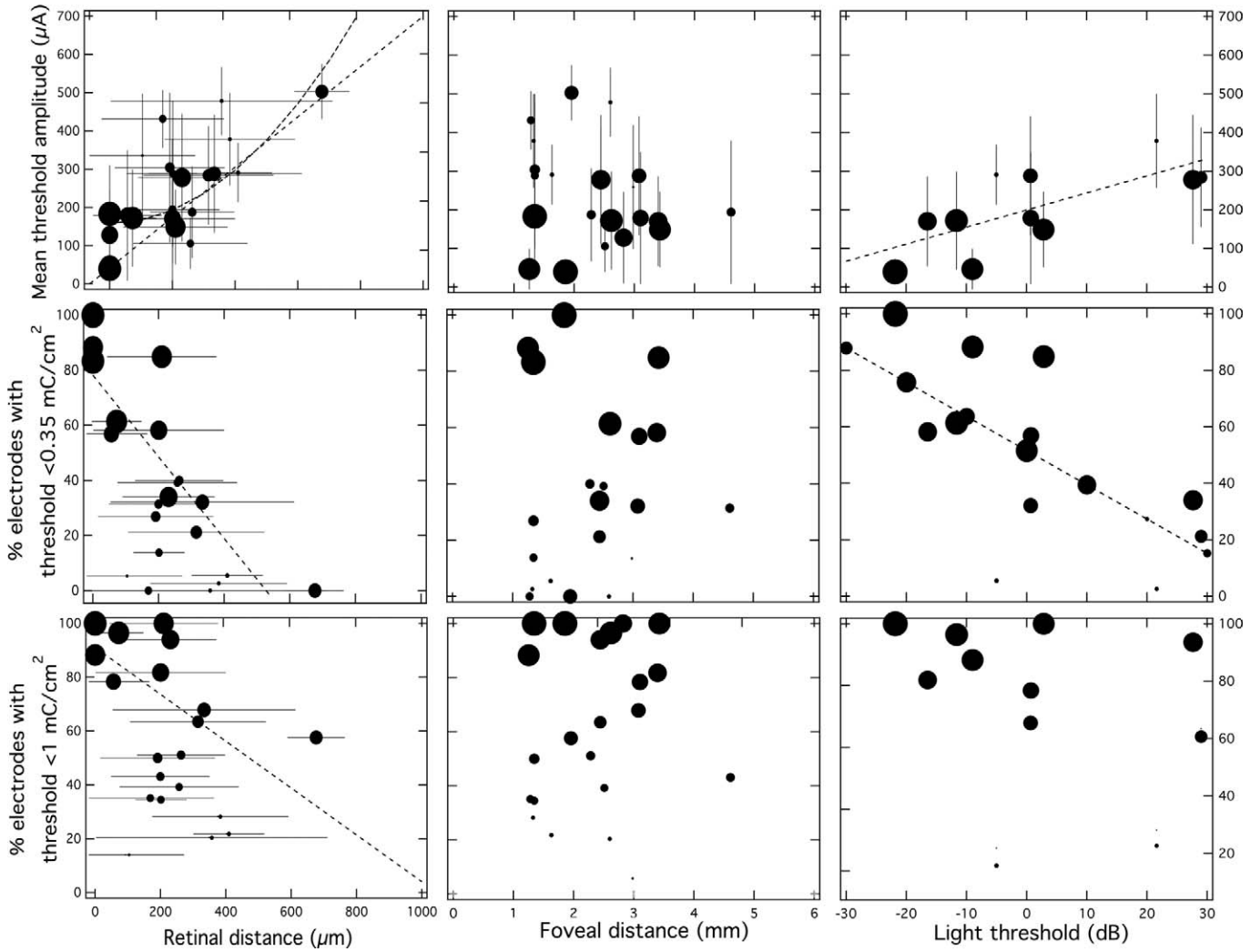

Figure 4. The effect of electrode–retina distance (*left*), electrode–fovea distance (*middle*), and light sensitivity (*right*) on mean electrode threshold (*top*), the percentage of electrodes with thresholds below 0.35 mC/cm^2 (*middle*), and the percentage below 1 mC/cm^2 (*bottom*). Linear regression (*dashed line*) showed that electrode–retina distance and monocular light threshold (measured in decibels with 0 dB = 3 (cd)(s)/m^2) correlate with mean threshold and percentage of electrodes with thresholds below 0.35 mC/cm^2. Square of distance fitting on mean threshold versus electrode–retina distance (**bold dashed line**) did not fit the data better than linear fitting. *Error bars* indicate ± standard deviation. Each data point is scaled to represent the number of electrodes included in the analysis for each subject (i.e., the largest circle represents inclusion of all electrodes in the array).

correlate with any of the response measures. Interestingly, there was no correlation with age or self-reported onset of blindness ($P > 0.5$; $n = 20$ subjects).

Electrode–fovea distance was the only explanatory variable that had no affect on any measure of threshold when linear regression was performed. Neither mean electrode–fovea distance nor mean geometric electrode–fovea distance correlated with any of the response measures when electrodes at all retinal distances were included ($P > 0.2$). In order to isolate the effect of foveal distance from the confounding factor of retinal distance, only electrodes touching the retina were included in the following additional analysis. Electrodes with thresholds below 25 μA had a mean foveal distance of 1777 ± 121 μm (n = 56 electrodes) compared with a mean foveal distance of 2318 ± 76 μm ($n = 299$ electrodes) for all electrodes with thresholds above 25 μA. Electrodes in contact with thresholds below 50 μA had a mean foveal distance of 1886 ± 81 μm ($n = 134$ electrodes) compared with a mean foveal distance of 2439 ± 93 μm (n = 216 electrodes) for all electrodes with

Table 3. Multivariate Modeling was Performed using a Standard Least Squares Method to Quantify the Extent to which Explanatory Variable Pairs could Predict Each Threshold Response Measure

	Mean Retinal Distance (μm) and Mean Foveal Distance (μm)		Mean Retinal Distance (μm) and Light Threshold (cd)(s)/m^2) (Implanted Eye)	
	R^2	P	R^2	P
Mean electrode threshold	0.57	0.02	0.87	0.0003
Electrodes (%) threshold <0.35 mC/cm^2	0.80	0.0003	0.80	0.002
Electrodes (%) threshold <1 mC/cm^2	0.79	0.01	0.63	0.02

Only explanatory variables with an overlap of more than five observations were included. Coefficient of determination (R^2) and significance of the trend (P-value) are given for each of the individual predictors. All measures of threshold showed a significant relationship ($P < 0.05$) when regressed against mean retinal and foveal distance, and mean retinal distance and light threshold of implanted eyes.

thresholds above 50 μA. For all electrodes in contact with the macula ($n = 270$ electrodes), 90.3% of electrodes had thresholds below 1 mC/cm^2, and 80.9% had thresholds below 0.35 mC/cm^2; mean threshold was 108 ± 7 μA. For extramacular electrodes in contact with the retina, these percentages decrease to 72.9% and 85.4%, respectively; mean threshold was 153 ± 16 ($n = 83$ electrodes).

The fact that the effect of increased ganglion cell density in the macula wasn't evident in linear regression isn't surprising since anatomical data shows a somatic density that is nonmonotonic as a function of foveal eccentricity. Data from this study done by Curcio and Allen[26] on the topology of the retina as well Argus II mean threshold data were plotted against foveal eccentricity (Fig. 5). The plots show that the ganglion cell (GC) density peak overlaps well with the mean threshold minima observed in the Argus II data, and that the two curves are inversely correlated ($P < 0.05$). This is an extremely positive finding as it provides some validation of a fundamental assumption made by the epiretinal approach, and grounds the clinical results to the larger body of literature on the anatomy and physiology of the retina.

Multivariate linear regression was reduced to bivariate analysis since only the effects of retinal distance and light threshold of the implanted eye were captured by the linear fit. Nonetheless, even when only these two variables are taken together they show a correlation with mean threshold ($R^2 = 0.87$; $P < 0.0005$) and percentage of available electrodes with thresholds below the 0.35 mC/cm^2 limit ($R^2 = 0.80$; $P < 0.005$) (Table 3).

Discussion

Effect of Electrode–Retina Distance on Threshold

Previous studies of retinal stimulation have quantified the functional dependence of threshold on electrode–retina distance in vitro using stimulating wires[27,28] and multielectrode arrays (Behrend MR, et al. *IOVS*. 2009;50:ARVO E-Abstract 4569).[29–30] A study in macaque retina using 9 to 15-μm diameter stimulating disc electrodes reported that threshold charge was inversely related with the square of the distance,[29] as would be expected from the fall off of the electric field as dictated by Coloumb's law. A study in salamander using the same sized electrodes as those used in the Argus II system (200-μm diameter) found a relationship that was slightly more linear ($y = ax^{1.69}$).[30] We found no significant difference between R^2 values of linear and square of distance fits across individuals (two-tailed paired Student's t-test, $P > 0.15$). One possible reason the square-of-distance relationship was evident in the study using smaller electrodes is because the spatial gradient of the field depends on disc diameter,[31] and the relative ratio of distance to recorded ganglion cell to stimulating electrode center was greater in the study using smaller discs (i.e., 5:1 vs. 2:1). The finding that 200-μm electrodes yield an exponent between one and two is also consistent with the fact that the field gradient can be linearly approximated in the near field (i.e., on the order of the disc radius). This dependence of electric field fall off on diameter also implies that the stimulus threshold using larger electrodes is less sensitive to distance. Therefore, although smaller electrodes may

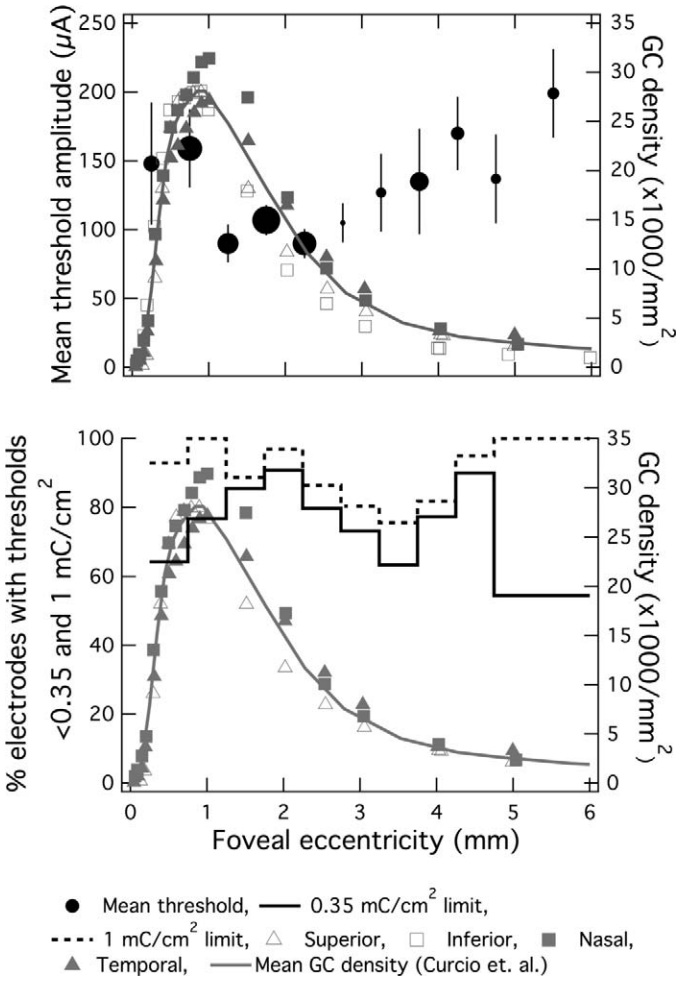

Figure 5. The effect of local ganglion cell density on stimulus threshold. (*top*) Mean threshold current amplitude (*black circles*) and ganglion cell density (*grey connected symbols* represent each retinal quadrant from Curcio and Allen's whole-mount study, *solid grey line* is the mean of these four quadrants) plotted against foveal eccentricity. Only electrodes in contact with the retina are included (in contrast with data plotted in Fig. 4), and electrodes are pooled across all subjects. Each *solid black circle* is representative of a 0.5 mm foveocentric bin with increasing diameter representative of electrode count for that bin. *Vertical bars* represent standard error. Mean threshold (*black circles* of varying diameter) and anatomical data correlated well ($P = 0.03$). (*bottom*) Percentage of electrodes with thresholds below 0.35 (*solid line*) and 1 mC/cm^2 (*dashed line*) plotted against foveal eccentricity (0.5-mm bins up to 4 mm from fovea centralis; 1-mm bins at eccentricities greater than 4 mm to ensure minimum sample size was 10 electrodes/bin). Bin count ranged from 11 to 63 electrodes.

provide increased spatial resolution in future prosthesis design due to increased electrode density and improved cell selectivity,[15,32] ensuring proximity will be even more critical.[33]

One advantage of a prosthetic compared with a gene therapy based approach is that since the latter is aimed at preserving the health and function of photoreceptor and retinal pigment epithelium (RPE) layers, individual therapies must be developed for specific genetic mutations, and RP consists of more than 200 different mutations. Disease genotype and extent of degeneration were not controlled for in this study. These variables along with individually defined psychophysical criteria should be considered regarding variance of functional fit of these data across subjects.

Effect of Electrode–Fovea Distance on Threshold

We believe this is the first report of the effect of foveal proximity on threshold. GC density is highest in the macula; however, these and other inner nuclear cells are laterally displaced from fovea centralis. Although electrodes with thresholds below these cutoff amplitudes were on average closer to the fovea compared with all other electrodes in contact with the retina, a nonmonotonic relationship between mean threshold and the percentage of electrodes with thresholds below 233 μA was observed when these threshold measures were plotted against foveocentric annular bin (Fig. 5; bins of electrodes contacting the retina were 0.5-mm wide; electrode count/bin ranged from 11 to 63 electrodes). Mean threshold exhibited a broad minimum ranging from 1 to 2.5 mm away from the fovea, with an absolute minima of 93 ± 14 μA for the 1- to 1.5-mm bin. The percentage of electrodes with thresholds below 233 μA had a maximum of 90.8% (57 of 63 electrodes) in the 1.5- to 2-mm bin. When testing was performed up to the 677 μA limit 100% of electrodes ($n = 43$) had thresholds in the 0.5- to 1-mm bin.

We believe this nonmonotonic relationship can be understood by comparing our data with that obtained in a whole-mount cell counting study in normal human retina. This postmortem study ($n = 6$) found a peak GC density of 27×10^3 cells/mm^2 at a foveal eccentricity of 1.08 ± 0.23 mm.[26] Data from this morphological study and threshold data of electrodes in contact with retinal tissue are plotted against foveal eccentricity (Fig. 5). There is a correlation between GC density and perceptual threshold (two-tailed paired Students's *t*-test, $P = 0.03$). The GC density maximum is within the same annular bin as the lowest mean threshold (90 ± 13 μA; 1–1.5 mm range). Taken together these results suggest that phosphene threshold is reduced when more cell somas are in the vicinity of the excitation field.

The fact that electrode threshold is higher in the foveal depression compared with the thicker rim is not surprising, nor should it be used as an argument against targeting macular placement. From implant design and surgical perspectives it is in fact encouraging to find that the range of the threshold minimum is fairly broad. Thresholds of the four bins in the 1- to 3-mm range were not significantly different; taken together these bins proximal to the rim are significantly lower when compared with bins for electrodes at all other eccentricities ($P < 0.01$). The area of the central 1 mm where a relative threshold increase is observed is just 12% of the total macular area (<3 mm). In fact, the ratio of the total electrode array grid area to the foveal depression is nominal, and ranges from 17.7 to 26.2 (depending on specific dimensions of the implanted array).

One concern with epiretinal stimulation has been that action potentials initiated by either the direct stimulation of axons, or the stimulation of these axons and the subsequent antidromic or orthodromic stimulation of corresponding GC's, would limit the ability to elicit punctuate percepts. The possibility of axonal stimulation has been in investigated by others. Modeling has shown that GC's have a slightly lower threshold (by 20% to 73% depending on neuronal model used) compared with their axons.[34] Experimental results in rabbit have shown that cathodic pulses yield a mean threshold for somatic stimulation, which is half that of axonal stimulation.[27] One reason why the cell soma may be a preferential site for spike initiation is because there is an increased number of voltage-sensitive sodium channels (Na_v 1.6) at the initial segment compared with the distribution along the rest of the fiber.[35,36] This theory is strongly supported by recent results in macaque,[29] salamander, (Behrend MR, et al. *IOVS*. 2009;50:ARVO E-Abstract 4569)[37] and rabbit (Fried SI, et al. *IOVS*. 2009;50:ARVO E-Abstract 4568) retina. Macular placement of the array should also help preferential stimulation of somas since axonal fiber tracts bundles present near the optic disc thin out into individual branches near the fovea, and it is known from neuromuscular stimulation that thicker mylenated axons have lower thresholds than thinner unmylenated ones.[38,39] Data presented here are in agreement with these findings. The fact that threshold can be predicted by GC density with 95% CI for electrodes touching the retina suggests the either cell somas or proximal corresponding initial segments are the primary target of extracellular stimulation as opposed to their axons.

It is possible that this correlation is weakened by the fact that degeneration in RP initiates in the midperiphery, and encroaches on the fovea with progression. Therefore, since we expect the fall off of the GC density profile to be exacerbated compared with normal retina,[21] it is impressive to see a correspondence between anatomical and psychophysical data in subjects with variations in disease genotype and progression.

Recent results from implanted Argus I and Argus II subjects showed percept shape was found to be more streak-like than punctate, and that steak angle matched the axonal cytoarchitecture. Given that these are human psychophysical data using the same implant it is worth reconciling the somatically- and axonally-driven hypotheses for percepts. Given the large size of electrodes compared with cell somas, and the use of amplitude coding to control brightness coupled with a narrow window of excitation of somas compared with axons, it is not surprising that percepts should be a product of the stimulation of both these elements. The conclusion drawn here is that while somas and axons are both stimulated (along with tens of different cell classes), somatic density and excitation drives phosphene shape when electrodes are closer to the foveal rim. While axonal studies were on 2 to 3 Argus I and Argus II subjects, this study used inclusion criteria based on date of implantation (i.e., a data cutoff point) and included the majority of subject's implanted in the trial. Prior studies were limited to subject availability and their ability to perform the task. The latter is adversely affected due to loss of spatial–motor coordination after years of blindness and cortical dormancy. Prior results on Argus II subjects showed that such spatial–motor coordination is better preserved in subjects with better light perception. It's possible that axonal studies focused on subjects with better residual vision because they could perform the task with some repeatability. In either case it is evident that the assumption that percepts are elicited solely by the stimulation of one of these elements or, for that matter, even a single class of cells (i.e., ganglion versus bipolar cells) is simplistic.

Effect of D-FST Light Threshold

For those blinded by advanced outer retinal degenerative disease it is not possible to use standard clinical electrophysiological (e.g., electro-retinography [ERG], multifocal electroretinography [mfERG]) and psychophysical (e.g., kinetic or static perimetry) testing as a method of quantitatively assessing vision and retinal health. The measurement of light thresh-

old to a full field stimulus has been used by others and was also used in this study. It has been shown in P23H transgenic line rats that the number of light-responsive ganglion cells decreases with disease progression.[40] In the same model it has also been shown that degeneration is accompanied not only by loss of photoreceptors, but also by anatomical remodeling and neural rewiring of the remnant inner retina.[1]

Electrophysiological studies have differed in their conclusions as per the effect of these changes on threshold. Some investigations reported electrical threshold was significantly higher in degenerate model (rd1) compared with wild-type mice.[41–44] However, a more recent study in P23H and S334Ter rats using pharmacologic blocking agents and a method of artifact subtraction intended to isolate the direct GC response, found no significant increase in electrical threshold up to postnatal day 750 (p750).[40] A likely hypothesis that has been proposed to account for this difference is that studies reporting relative threshold increases stimulated various types of cells in the inner and outer retina.[30] Since synaptic connections to the GC layer are compromised as degeneration advances, a decrease in action potential spike threshold was observed. This is consistent with the fact that response latencies were comparatively long (>3 ms), envelopes of reverberating spiking lasting greater than 400 ms were observed, and that all responses were abolished with the application of blocking agents inhibiting indirect presynaptic excitation of GC's.[30,45,46] In contrast, reports of thresholds of short latency responses (<1 ms) using small disc electrodes[15] and conical electrodes[32] were shown to persist with application of these agents indicating direct GC stimulation. These results are consistent with the fact that remodeling affects the inner retinal network, but that GC structure[47] and cell membrane properties[48] remain relatively unchanged.

The fact that we observe a positive correlation between electrical threshold and light threshold in implanted subjects suggests presynaptic cells are stimulated and contribute to the percept. This is predicted by prior work showing that while small diameter conical electrodes stimulating with short pulses (0.15 ms) target ganglion cells,[32] longer pulses (>1 ms) target amacrine and bipolar cells because of the longer chronaxies of graded potential cells.[49,50] The 0.45 ms cathodic-first biphasic pulses used in this study are above the cutoff for direct GC stimulation. The finding in Argus II subjects is also in agreement with a past report of increased acute stimulation thresholds in five profound RP subjects compared with one healthy, and with a report where threshold was found to be lower in the same subject in areas visibly adversely affected by disease compared with the rest of the tissue.[51,52] Because the comparatively large (50–400 μm) electrodes have stimulating fields that penetrate multiple inner and outer retinal layers, it is certainly possible that loss of synaptic integrity between these layers (along with many other effects associated with degeneration) caused an increase in threshold. Nevertheless, the fact that the threshold of direct GC stimulation does not decrease over time[40] suggests that future prostheses employing smaller stimulating electrodes are feasible and may be more independent of disease progression compared with larger electrodes.

We believe that D-FST light threshold is predicative of electrical threshold because it is a measure of underlying viability and preservation of structure. Given differences in genotype, pathology, and advancement in implanted subjects it is not surprising that there is no relationship between threshold and either age at implantation or self-reported number of years blind. Taken together, these results suggest that subjects should not be excluded as candidates for implantation based on either age or number of years blind. The D-FST light threshold test provides sufficient physiological assessment with regard to informing clinicians and patients.

Conclusion

It has been shown by others that electrode–retina distance strongly affects threshold. Our results show that this is the most important factor of those investigated here. We conclude that macular placement of the array is critical for two reasons. Firstly, the fovea is the center of both high-acuity vision and cortical-based attention in the normally sighted. Secondly, ganglion cell density is highest in the macula.[18,26] It has been shown that the majority of Argus II subjects with comparatively good bare light perception can successfully integrate native and artificial vision in a high-contrast spatial-motor task (Ahuja A, *IOVS*. 2010;51:ARVO E-Abstract 4322; McMahon MJ, et al. *IOVS*. 2009;50:ARVO E-Abstract 4589; Ahuja A, et al. *IOVS*. 2009;50:ARVO E-Abstract 4590), and that D-FST measured light sensitivity of implanted eyes does not significantly decrease when compared with fellow eyes over a 2 year time period post implant (Dagnelie G, et al. *IOVS*. 2010;51:ARVO E-Abstract 3029). In the absence of medical reasons to the contrary, these

results taken together with the direct relationship between electrical perceptual threshold and light threshold support intervention earlier in the time course of disease onset (i.e., patients with better residual vision are good candidates for the Argus II prosthesis). The current visual acuity inclusion criterion for the clinical trial was that subjects score below 2.9 LogMAR on grating acuity testing. According to the electrode size and pitch the theoretical limit of the system is 1.9 LogMAR. Determination of exactly how early surgical implantation can be justified, however, should be based on more than visual acuity as there are many other tests that mimic real world conditions that should be included in assessment (e.g., orientation and mobility, activities of daily living, and quality of life).[53] Providing an exact time point will require further clinical study, patient training, and follow up.

When analyzing data from all subjects who have a range of light threshold levels, we found that 90.3% of electrodes placed in direct contact with the retina and within 3 mm of fovea centralis had thresholds below 1 mC/cm^2, and 80.9% had thresholds below 0.35 mC/cm^2. Therefore, while light threshold measurement can be used by clinicians and researchers prior to implantation, placing the array in proximity with the retinal surface and in the macula is paramount, and allows for a high percentage of electrodes to elicit phosphenes in those blinded by advanced RP.

It should be possible to use smaller electrodes with more consistent placement and apposition. Acute stimulation studies in those with advanced RP performed by another group employing an epiretinal approach showed that percepts could be elicited below safe charge injection limits with 100-μm diameter discs.[54,55] Based on the average minimum threshold for optimally placed electrodes in Argus II subjects, it should be possible to safely use 130-μm diameter electrodes when employing a maximum charge density of 0.35 mC/cm^2, and 45-μm diameter electrodes when employing a maximum charge density of 1 mC/cm^2. Such improvements in device design and surgical placement have the potential to provide even higher resolution in future generation implants for those blinded by outer retinal dystrophies.

Acknowledgments

Disclosure: **A.K. Ahuja,** Second Sight Medical Products (F); **J. Yeoh,** None; **J.D. Dorn,** Second Sight Medical Products (F, I, E, P, R); **A. Caspi,** Second Sight Medical Products (F, I, E, P, R); **V. Wuyyuru,** Second Sight Medical Products (F, I, E, P, R); **M.J. McMahon,** Second Sight Medical Products (F, I); **M.S. Humayun,** Second Sight Medical Products (F, I, R); **R.J. Greenberg,** Second Sight Medical Products (F, I, E, P, R); **L. daCruz,** Second Sight Medical Products (F, R); **Argus II Study Group,** Second Sight Medical Products (F) This work was supported by a grant from the National Institute of Health (5R01EY12893).

References

1. Marc RE, Jones BW, Watt CB, Strettoi E. Neural remodeling in retinal degeneration. *Prog Retin Eye Res*. 2003(5);22:607–655.
2. Santos A, Humayun MS, de Juan E, Jr, et al. Preservation of the inner retina in retinitis pigmentosa. A morphometric analysis. *Arch Ophthalmol*. 1997(4);22:511–515.
3. Stone JL, Barlow WE, Humayun MS, de Juan E, Jr, Milam AH. Morphometric analysis of macular photoreceptors and ganglion cells in retinas with retinitis pigmentosa. *Arch Ophthalmol*. 1992(11);110:1634–1639.
4. Rizzo JF, 3rd, Wyatt J, Loewenstein J, Kelly S, Shire D. Perceptual efficacy of electrical stimulation of human retina with a microelectrode array during short-term surgical trials. *Invest Ophthalmol Vis Sci*. 2003(12);44:5362–5369.
5. Zrenner E, Stett A, Weiss S, et al. Can subretinal microphotodiodes successfully replace degenerated photoreceptors? *Vision Res*. 1999(15);39:2555–2567.
6. Humayun MS, de Juan E, Jr, Dagnelie G, Greenberg RJ, Propst RH, Phillips DH. Visual perception elicited by electrical stimulation of retina in blind humans. *Arch Ophthalmol*. 1996(1);114:40–46.
7. Jacobson SG, Yagasaki K, Feuer WJ, Roman AJ. Interocular asymmetry of visual function in heterozygotes of X-linked retinitis pigmentosa. *Exp Eye Res*. 1989(5);48:679–691.
8. Behrend M, Ahuja A, Humayun M, Chow R, Weiland J. Resolution of the Epiretinal Prosthesis is not Limited by Electrode Size. *IEEE Trans Neural Syst Rehabil Eng*. 2011(4);19:436–442.
9. Humayun MS, Dorn JD, Ahuja AK, et al. Preliminary 6 month results from the argus™ ii

epiretinal prosthesis feasibility study. *Conf Proc IEEE Eng Med Biol Soc*. 2009;1:4566–4568.
10. Behrend MR, Ahuja AK, Humayun MS, Weiland JD, Chow RH. Selective labeling of retinal ganglion cells with calcium indicators by retrograde loading in vitro. *J Neurosci Methods*. 2009(2);178:166–172.
11. McCreery DB, Agnew WF, Yuen TG, Bullara LA. Comparison of neural damage induced by electrical stimulation with faradaic and capacitor electrodes. *Ann Biomed Eng*. 1988(5);16:463–481.
12. Roblee LS, Rose TL. *Electrochemical guidelines for selection of protocols and electrode materials for neural stimulation*. in *Neural Prosthesis: Fundamental Studies*, Agnew WF, McCreery DB, Editors. 1990: Englewood Cliffs.
13. Fried SI, Hsueh HA, Werblin FS. A method for generating precise temporal patterns of retinal spiking using prosthetic stimulation. *J Neurophysiol*. 2006(2);95:970–978.
14. Safir A, McDonald MB, Friedlander MH, Granet NS, Werblin TP, Kaufman HE. Compensating for thermally caused dimensional changes in the cryolathe. *Ophthalmic surgery*. 1984(4);15:306–309.
15. Sekirnjak C, Hottowy P, Sher A, Dabrowski W, Litke AM, Chichilnisky EJ. Electrical stimulation of mammalian retinal ganglion cells with multielectrode arrays. *J Neurophysiol*. 2006(6);95:3311–3327.
16. de Balthasar C, Patel S, Roy A, et al. Factors affecting perceptual thresholds in epiretinal prostheses. *Invest Ophthalmol Vis Sci*. 2008(6);49:2303–2314.
17. Caspi A, Dorn JD, McClure KH, Humayun MS, Greenberg RJ, McMahon MJ. Feasibility study of a retinal prosthesis: spatial vision with a 16-electrode implant. *Arch Ophthalmol*. 2009(4);127:398–401.
18. Rohrschneider K. Determination of the location of the fovea on the fundus. *Invest Ophthalmol Vis Sci*. 2004(9);45:3257–3258.
19. Drasdo N, Fowler CW. Non-linear projection of the retinal image in a wide-angle schematic eye. *Br J Ophthalmol*. 1974(8);58:709–714.
20. Aleman TS, Cideciyan AV, Sumaroka A, et al. Inner retinal abnormalities in X-linked retinitis pigmentosa with RPGR mutations. *Invest Ophthalmol Vis Sci*. 2007(10);48:4759–4765.
21. Aleman TS, Cideciyan AV, Sumaroka A, et al. Retinal laminar architecture in human retinitis pigmentosa caused by Rhodopsin gene mutations. *Invest Ophthalmol Vis Sci*. 2008(4);49:1580–1590.
22. Roman AJ, Cideciyan AV, Aleman TS, Jacobson SG. Full-field stimulus testing (FST) to quantify visual perception in severely blind candidates for treatment trials. *Physiol Meas*. 2007(8);28:N51–N56.
23. Roman AJ, Schwartz SB, Aleman TS, et al. Quantifying rod photoreceptor-mediated vision in retinal degenerations: dark-adapted thresholds as outcome measures. *Exp Eye Res*. 2005(2);80:259–272.
24. Klein M, Birch DG. Psychophysical assessment of low visual function in patients with retinal degenerative diseases (RDDs) with the Diagnosys full-field stimulus threshold (D-FST). *Doc Ophthalmol*. 2009(3);119:217–224.
25. Roman AJ, Schwartz SB, Aleman TS, et al. Quantifying rod photoreceptor-mediated vision in retinal degenerations: dark-adapted thresholds as outcome measures. *Exp Eye Res*. 2005(2);80:259–272.
26. Curcio CA, Allen KA. Topography of ganglion cells in human retina. *J Comp Neurol*. 1990(1);300:5–25.
27. Jensen RJ, Rizzo JF, 3rd, Ziv OR, Grumet A, Wyatt J. Thresholds for activation of rabbit retinal ganglion cells with an ultrafine, extracellular microelectrode. *Invest Ophthalmol Vis Sci*. 2003(8);44:3533–3543.
28. Ziv OR, Rizzo JF, Jensen RJ. In vitro activation of retinal cells: estimating location of stimulated cell by using a mathematical model. *J Neural Eng*. 2005(1);2:S5–S15.
29. Sekirnjak C, Hottowy P, Sher A, Dabrowski W, Litke AM, Chichilnisky EJ. High-resolution electrical stimulation of primate retina for epiretinal implant design. *J Neurosci*. 2008(17);28:4446–4456.
30. Ahuja AK, Behrend MR, Kuroda M, Humayun MS, Weiland JD. An in vitro model of a retinal prosthesis. *IEEE Trans Biomed Eng*. 2008(6);55:1744–1753.
31. Forster RJ. *Microelectrodes - Retrospect and Prospect*. in *Electroanalytical Methods*. Bard AJ, Stratman, M Editors. 2005, Wiley Publishing.
32. Fried SI, Hsueh HA, Werblin FS. A method for generating precise temporal patterns of retinal spiking using prosthetic stimulation. *J Neurophysiol*. 2006.(2);95:970–978.
33. Palanker D, Huie P, Vankov A, et al. Migration of retinal cells through a perforated membrane: implications for a high-resolution prosthesis. *Invest Ophthalmol Vis Sci*. 2004(9);45:3266–3270.
34. Greenberg RJ, Velte TJ, Scarlatis GN, de Juan E, Jr. A computational model of electrical stimula-

tion of the retinal ganglion cell. *IEEE Trans Biomed Eng*. 1999(5);46:505–514.
35. Boiko T, Van Wart A, Caldwell JH, Levinson SR, Trimmer JS, Matthews G. Functional specialization of the axon initial segment by isoform-specific sodium channel targeting. *J Neurosci*. 2003(6);23:2306–2313.
36. Schiefer MA, Grill WM. Sites of neuronal excitation by epiretinal electrical stimulation. *IEEE Trans Neural Syst Rehabil Eng*. 2006(1); 14:5–13.
37. Behrend M, Ahuja A, Humayun M, Chow R, Weiland J. Resolution of the Epiretinal Prosthesis is not Limited by Electrode Size. *IEEE Trans Neural Syst Rehabil Eng*. 2011(4);19:436–442.
38. Ranck JB, Jr. Which elements are excited in electrical stimulation of mammalian central nervous system: a review. *Brain Res*. 1975(3);98:417–440.
39. Fang ZP, Mortimer JT. A method to effect physiological recruitment order in electrically activated muscle. *IEEE Trans Biomed Eng*. 1991(2);38:175–179.
40. Sekirnjak C, Hulse C, Jepson LH, et al. Loss of responses to visual but not electrical stimulation in ganglion cells of rats with severe photoreceptor degeneration. *J Neurophysiol*. 2009(6);102:3260–3209.
41. O'Hearn TM, Sadda SR, Weiland JD, Maia M, Margalit E, Humayun MS. Electrical stimulation in normal and retinal degeneration (rd1) isolated mouse retina. *Vision Res*. 2006(19);46:3198–3204.
42. Suzuki S, Humayun MS, Weiland JD, et al. Comparison of electrical stimulation thresholds in normal and retinal degenerated mouse retina. *Jpn J Ophthalmol*. 2004(4);48:345–9.
43. Chen SJ, Mahadevappa M, Roizenblatt R, Weiland J, Humayun M. Neural responses elicited by electrical stimulation of the retina. *Trans Am Ophthalmol Soc*. 2006;104:252–259.
44. Jensen RJ, Rizzo JF III. Activation of retinal ganglion cells in wild-type and rd1 mice through electrical stimulation of the retinal neural network. *Vision Res*. 2008(14);48:1562–1568.
45. Crapper DR, Noell WK. Retinal Excitation and Inhibition from Direct Electrical Stimulation. *J Neurophysiol*. 1963;26:924–947.
46. Jensen RJ, Ziv OR, Rizzo JF III. Thresholds for activation of rabbit retinal ganglion cells with relatively large, extracellular microelectrodes. *Invest Ophthalmol Vis Sci*. 2005(4);46:1486–1496.
47. Margolis DJ, Newkirk G, Euler T, Detwiler PB. Functional stability of retinal ganglion cells after degeneration-induced changes in synaptic input. *J Neurosci*. 2008(25);28:6526–6536.
48. Mazzoni F, Novelli E, Strettoi E. Retinal ganglion cells survive and maintain normal dendritic morphology in a mouse model of inherited photoreceptor degeneration. *J Neurosci*. 2008(52);28:14282–14292.
49. Greenberg R. *Analysis of electrical stimulation of the vertbrate retina - work towards a retinal prosthesis*. Baltimore, Maryland: Johns Hopkins University; 1998 Dissertation.
50. Margalit E, Thoreson WB. Inner retinal mechanisms engaged by retinal electrical stimulation. *Invest Ophthalmol Vis Sci*. 2006(6);47:2606–2612.
51. Rizzo JF III, Wyatt J, Loewenstein J, Kelly S, Shire D. Methods and perceptual thresholds for short-term electrical stimulation of human retina with microelectrode arrays. *Invest Ophthalmol Vis Sci*. 2003(12);44:5355–5361.
52. Humayun MS, de Juan E, Jr, Weiland JD, et al. Pattern electrical stimulation of the human retina. *Vision Res*. 1999(15);39:2569–2576.
53. Lepri BP. Is acuity enough? Other considerations in clinical investigations of visual prostheses. *J Neural Eng*. 2009(3);6:035003.
54. Klauke S, Goertz M, Rein S, et al. Stimulation with a wireless intraocular epiretinal implant elicits visual percepts in blind humans. *Invest Ophthalmol Vis Sci*. 2011(1);52:449–455.
55. Roessler G, Laube T, Brockmann C, et al. Implantation and explantation of a wireless epiretinal retina implant device: observations during the EPIRET3 prospective clinical trial. *Invest Ophthalmol Vis Sci*. 2009(6);50:3003–3008.